JOURNAL OF COMPUTATIONAL PHYSICS 65, 46–56 (1986)

Steady Laminar Forced Convection from a Circular Cylinder

HAMID JAFROUDI AND H. T. YANG

Department of Aerospace Engineering, University of Southern California, Los Angeles, California 90089-0192

Received February 22, 1985; revised September 13, 1985

The Navier–Stokes and energy equations for the steady, incompressible, laminar flow past a circular cylinder at constant temperature are solved by expressing the temperature as well as the stream function in truncated Fourier series. The partial differential equations are reduced to a system of simultaneous ordinary differential equations, which are then numerically integrated. The Reynolds numbers Re, based on the diameter, range from 1 to 40; and the Prandtl number Pr for air is taken as 0.72. Navier–Stokes solutions at large distances from the cylinder obtained by coordinate expansion are used as velocity boundary conditions at infinity. This type of boundary condition at infinity is shown to be more appropriate than the free stream or Oseen approximation. Heat transfer in terms of local and mean Nusselt numbers are computed and compared with available numerical and experimental data.

1. INTRODUCTION

As a sequel to the authors' previous work [10], the temperature field and heat transfer from a circular cylinder in steady, laminar, incompressible flow up to Reynolds number 40 are obtained. The partial differential equations are reduced to ordinary ones by Fourier expansion of the stream function and temperature. The Navier–Stokes solution at large distances [3] is used as the far field velocity boundary conditions. This type of boundary conditions is shown to be more appropriate than the free stream or Oseen approximations used by most authors. See Table 1 of Fornberg [8], where the far field velocity boundary condition has been considered in detail. Fornberg recommended usage of the zero normal derivative boundary condition for Reynolds numbers up to 40; and the "mixed condition" for higher Reynolds numbers. We feel, however, that Chang's asymptotic solution [3] could be consistently used for both Reynolds number ranges. For the temperature boundary condition at infinity, the situation is far less critical; and the free-stream condition may be used without any problem.

0021-9991/86 $3.00

2. Mathematical Formulations

We consider 2-dimensional uniform free-stream with velocity U_∞ and temperature T_∞ past a circular cylinder. The surface temperature T_w is assumed to be uniform. The density ρ, kinematic viscosity ν, thermal conductivity k and specific heat c_p of the air will be regarded as constants. Heating of the fluid by viscous dissipation from the cylinder is neglected. The flow is also assumed symmetrical about the axis of the cylinder for the Reynolds numbers up to 40.

The vorticity transport equation in two dimensions is, nondimensionalized with respect to free stream speed and the radius of cylinder, a

$$\nabla^4\psi + \frac{\mathrm{Re}_a}{r}\left(\frac{\partial\psi}{\partial\theta}\frac{\partial}{\partial r} - \frac{\partial\psi}{\partial r}\frac{\partial}{\partial\theta}\right)\nabla^2\psi = 0 \tag{1}$$

where the velocity components in polar coordinates are derivable from stream function

$$u_r(r,\theta) = -\frac{1}{r}\frac{\partial\psi}{\partial\theta} \tag{2}$$

$$u_\theta(r,\theta) = \frac{\partial\psi}{\partial r} \tag{3}$$

The vorticity is

$$\omega(r,\theta) = \nabla^2\psi. \tag{4}$$

The Reynolds number based on the radius, a, of the cylinder is

$$\mathrm{Re}_a = \frac{U_\infty a}{\nu}. \tag{5}$$

The energy equation in nondimensional form is

$$\nabla^2 T^* + \frac{\mathrm{Re}_a\,\mathrm{Pr}}{r}\left(\frac{\partial\psi}{\partial\theta}\frac{\partial T^*}{\partial r} - \frac{\partial\psi}{\partial r}\frac{\partial T^*}{\partial\theta}\right) = 0 \tag{6}$$

where Prandtl number Pr and dimensionless temperature T^* are

$$\mathrm{Pr} = \mu c_p/k = \rho\nu c_p/k \tag{7}$$

$$T^* = \frac{T - T_\infty}{T_w - T_\infty}. \tag{8}$$

The no-slip and uniform surface temperature boundary conditions are

$$\psi(r,\theta) = 0, \tag{9}$$

$$\frac{\partial \psi}{\partial r}(r, \theta) = 0, \tag{10}$$

$$T^*(r, \theta) = 1 \tag{11}$$

at $r = 1$, and uniform free-stream conditions

$$\psi(r, \theta) \to r \sin \theta \tag{12}$$

$$T^*(r, \theta) \to 0 \tag{13}$$

as $r \to \infty$.

Fourth- and second-order partial differential equations (1) and (6), with boundary conditions (9)–(13), describe the flow and temperature fields under consideration.

3. Method of Solution

The method of series truncation is employed for the solution of the systems (1), (6), and (9)–(13). The stream function and temperature are expanded as Fourier series

$$\psi(r, \theta) = \sum_{n=1}^{\infty} g_n(r) \sin n\theta \tag{14}$$

$$T^*(r, \theta) = \sum_{l=0}^{\infty} f_l(r) \cos l\theta \tag{15}$$

where functions $g_n(r)$ and $f_l(r)$ are to be determined. Substitution of (14) into (1) yields a set of nonlinear ordinary differential equations for vorticity-transport as in Jafroudi and Yang [10].

Substitution of (14) and (15) into (6) yields a set of linear equations for temperature

$$\sum_{l=0}^{N} \left[f_l'' + \frac{1}{r} f_l' - \frac{l^2}{r^2} f_l \right] \cos l\theta + \frac{\mathrm{Re}_a \, \mathrm{Pr}}{r} \sum_{l=0}^{N} \sum_{m=1}^{N} [m f_l' g_m \cos l\theta \sin m\theta]$$
$$+ \sum_{l=0}^{N} \sum_{m=1}^{N} [m g_m' f_l \sin l\theta \sin m\theta] = 0 \tag{16}$$

with the boundary conditions

$$f_0(1) = 1, \tag{17}$$

$$f_l(1) = 0, \qquad l = 1, 2, \ldots, N \tag{18}$$

$$f_l(r) = 0, \qquad l = 0, 1, 2, \ldots, N \text{ as } r \to \infty \tag{19}$$

where prime denotes differentiation with respect to r. The system of second-order ordinary differential equations (16) subjected to boundary conditions (17), (18), and (19) is to be numerically integrated to obtain the temperature.

In this work, ten terms of the Fourier series were employed for velocity and temperature, respectively.

Chang's [3] outer matched asymptotic expansion was used for the third-order velocity boundary conditions at large distance. They are given in [10] as

$$g_1(r) = r + \frac{\ln \varepsilon}{r}\left[\frac{3^{1/2} C_D^3 \operatorname{Re}_a}{16\pi^2} - \frac{C_D^2}{2\pi^2}\right] - \left(\frac{\operatorname{Re}_a}{2\pi}\right)^{1/2} \frac{C_D^2}{r^{1/2}} \frac{2}{3\pi} - \frac{C_D}{\pi} \tag{20}$$

$$g_n(r) = (-1)^n \left[\left(\frac{\operatorname{Re}_a}{2\pi r}\right)^{1/2} \frac{2nC_D^2}{(4n^2-1)\pi} + \frac{C_D}{n\pi}\right], \quad n = 2, 3, \ldots, \tag{21}$$

where

$$\varepsilon = a/R$$

with R an artificial length scale such that ε is a small parameter.

The temperature boundary conditions (19) remain unchanged. Apelt [1] and Takaisi [15] have demonstrated that applying velocity boundary conditions (12) leads to substantial inaccuracies in the results, unless the radial distance at which the conditions (12) are imposed is very large. This matter will be illustrated in Fig. 3 and discussed in Section 6.

4. Surface Quantities

The heat transfer expressed in terms of the Nusselt number, $\overline{Nu}$, is defined as

$$\overline{Nu} = -\int_0^{2\pi} k\left(\frac{\partial T}{\partial r}\right)_{r=a} a\, d\theta \Big/ 2\pi a\left[k\frac{T_W - T_\infty}{2a}\right]. \tag{22}$$

In the present formulation, it simplifies to

$$\overline{Nu} = -2f_0'(1) \tag{23}$$

It is seen from Eq. (23) that only the first term in the Fourier expansion (15) contributes to the Nusselt number. The value of $f_0(1)$ and its derivative do change as the number of terms in expansion (15) is increased.

5. Numerical Method

The efficient and simple initial value adjusting method with interval decomposition for the solution of nonlinear multipoint boundary value problem

(MPBVP) of nonlinear ordinary differential equations by Ojika [14], used in [10], has been adopted for the present two-point boundary value problem.

6. Results and Discussions

Numerical Results

Computations have been carried out for the study of the incompressible, laminar flow past a circular cylinder at constant temperature for Reynolds numbers ranging from 1 to 40 and Prandtl number of 0.72 for air.

In numerical computations the selection of outer boundary conditions at infinity is very crucial. See Fornberg [8]. Using the Oseen model and our numerical method, we plotted the component of tangential velocity at the angle of $\theta = \pi/2$ in Fig. 1 for $\mathrm{Re} = 1$ and radii r_∞ equal to 41, 61, and 91 based on unit radius of the cylinder. It is seen in Fig. 1 that, by increasing r_∞ to 61 or 91, the profiles of tangential velocity for different radii do not coincide. This clearly shows that $r_\infty = 41$ is not far enough to impose the outer boundary conditions. The problem of outer boundary condition may be alleviated by using Chang's [3] third-order coordinate expansion of the Navier–Stokes solutions at large distances from the cylinder. As a test of accuracy of the solution obtained from these boundary conditions, we plotted the component of tangential velocity at the angle $\theta = \pi/2$ in Fig. 2 for $\mathrm{Re} = 1$ and three radii r_∞ of 41, 61, and 91. In this figure, the results of outer expansion (3)

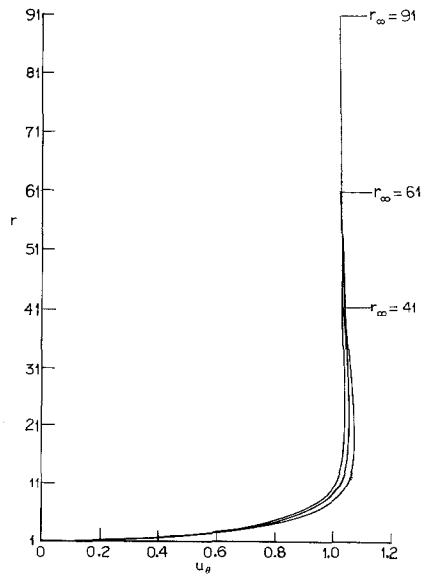

FIG. 1. Tangential velocity profiles at $\theta = \pi/2$ and $\mathrm{Re} = 1$ Oseen boundary conditions at $r_\infty = 41$, 61, and 91.

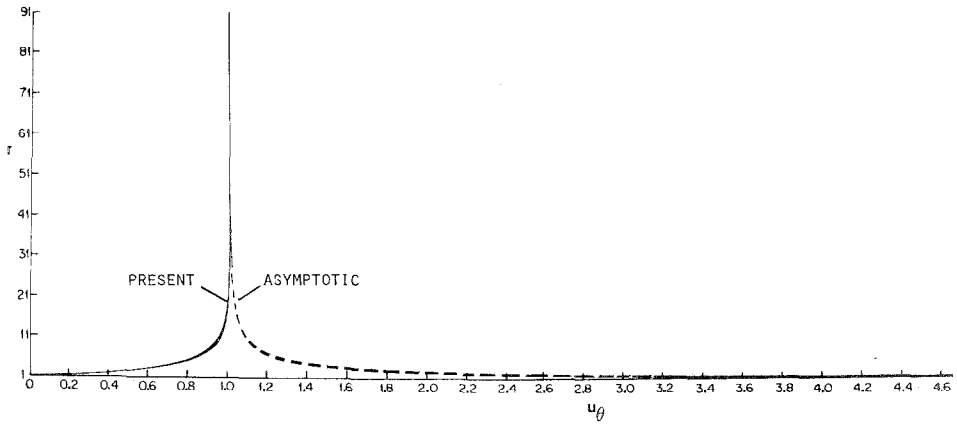

FIG. 2. Matching of computed tangential velocity profiles with far field Navier–Stokes solutions at $\theta = \pi/2$, Re = 1, and $r_\infty = 41$, 61, and 91.

with (14), (20), and (21) are also plotted from the outer distance to the surface of the cylinder to show where the matching occurs. This figure shows that there are no appreciable differences among the results of tangential velocity for three different radii r_∞. Using uniform flow condition or Oseen flow as outer boundary conditions forced some mass into the inner region in order to conserve mass, as seen in Fig. 1. But by using the higher order approximation in outer boundary, the mass is

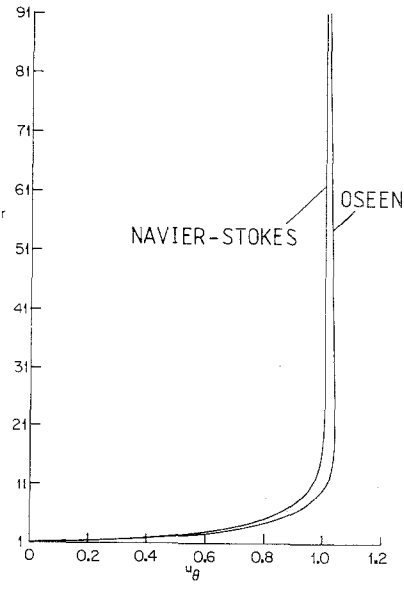

FIG. 3. Comparison of tangential velocity profiles at $\theta = \pi/2$, Re = 1, $r_\infty = 91$, with Oseen and far field Navier–Stokes solutions as boundary conditions.

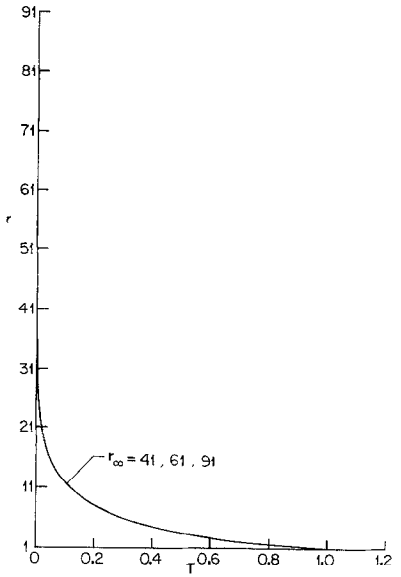

FIG. 4. Temperature profiles at $\theta = \pi/2$, Re = 1, Pr = 0.72, and $r_\infty = 41, 61$, and 91.

automatically conserved, and mass does not need to be forced inward, see Fig. 2. The component of tangential velocity is also plotted in Fig. 3 for $r_\infty = 91$ and Re = 1. The outer boundary conditions are chosen from Oseen flow and Chang's solution to the third order. Comparison of these two profiles shows that much larger distances, r_∞ are required for the imposing of Oseen flow as an outer boundary condition.

In Fig. 4 three temperature profiles at $\theta = \pi/2$ for Re = 1 and Pr = 0.72 are plotted against radial distances of 41, 61, and 91 from the center of a unit radius cylinder. The uniform temperature T_∞ is used as the outer boundary condition (19) for the energy equation (16). It is seen that the three temperature profiles

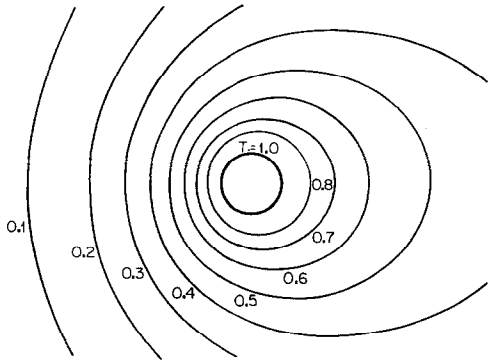

FIG. 5. Isotherms from the tenth truncation at Re = 1 and Pr = 0.72.

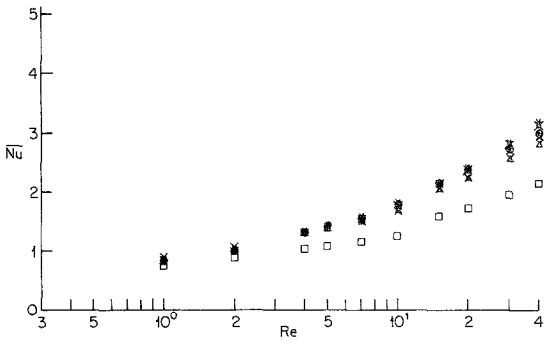

FIG. 6. Average Nusselt number versus Reynolds number (Pr = 0.72) from different truncations: second (□), third (△), fourth (×), fifth (◇), sixth (+), seventh (○), eight (⊠), ninth (z), and tenth (*).

corresponding to the three radii are essentially the same. This means that the uniform temperature condition T_∞ as the far field boundary condition is adequate. On the other hand, more refined far field boundary conditions should be used for the vorticity equation as discussed previously.

Note that the distance where the outer boundary conditions are imposed decreases as flow Reynolds number increases. As the viscous layer next to the cylinder surface becomes thinner at larger Reynolds numbers, shorter distances could be employed to match the far field conditions.

After all these trials, we selected the third-order outer expansions (20) and (21) instead of the uniform flow condition (12) for vorticity equation (1) and uniform temperature condition (19) for energy equation (6). For expediency, we chose an outer boundary of 91 for Reynolds numbers between 1 and 10; and 41 for Reynolds numbers between 10 and 40 and higher. To be consistent, we also used the same distance r_∞, at which the outer boundary condition is imposed, for all truncations for a given Reynolds number and Pr = 0.72.

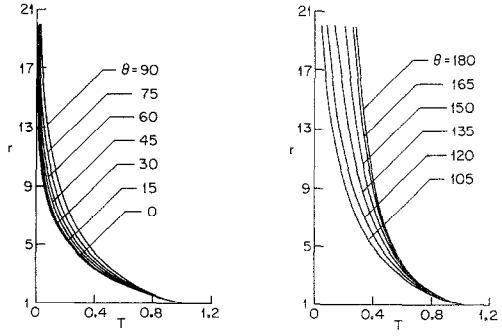

FIG. 7. Temperature profiles from the tenth truncation at Re = 1 and Pr = 0.72.

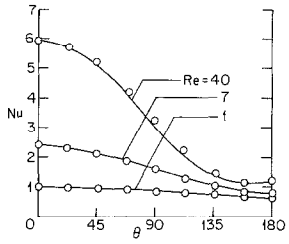

FIG. 8. Local Nusselt number from the tenth truncation (−) at Re = 1, 7, and 40, and Pr = 0.72, and (○) Dennis *et al.* (1968).

Because of the capacity limitation of the computer, we employed only ten terms of Fourier series for velocity and temperature, respectively. More terms in the Fourier series would enhance the accuracy of the results for higher Reynolds numbers. Since the tenth truncation yields the best obtainable approximation in the present work, the stream function (14), tangential and radial velocity profiles (2) and (3), and temperature profiles (15) have been so computed. Figure 5 shows the isotherms for Re = 1, and Pr = 0.72. Figure 6 shows the average Nusselt number $\bar{N}u$ versus Reynolds number Re from the second to tenth truncations. The temperature profile (15) for various angles are illustrated in Fig. 7 for Re = 1 and Pr = 0.72.

Comparison of Results

In Fig. 8, we plotted the local Nusselt number from the tenth truncation of the present work and the numerical computation of Dennis, Hudson and Smith [6] for Reynolds number 1, 7, and 40 and Pr = 0.73. The agreements are excellent for all Reynolds numbers. Also the local Nusselt numbers at Reynolds numbers 20 and 30 are plotted in Fig. 9 along with the experimental data of Eckert and Soehngen [7]. This figure shows that the trend of present semi analytic—numerical and experimental data are the same up to $\theta \simeq 128°$, but after this angle, the data shows higher value for Nusselt number when it approaches the wake of the cylinder.

The average Nusselt number is given in Table I. The result of present study shows good agreement with numerical solution of Dennis *et al.* and Apelt and Ledwich [2].

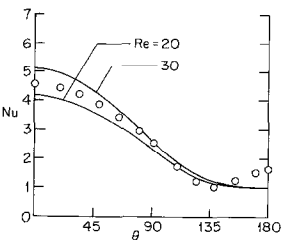

FIG. 9. Comparison of local Nusselt number from the tenth truncation (−) at Re = 20, 30, and Pr = 0.72 with experiments of (○) Eckert and Soehngen (1952) at Re = 23, Pr = 0.72.

TABLE I

Comparison of Average Nusselt Number from the Tenth Truncation with Existing Numerical Solutions

Re	Apelt and Ledwich (1979)	Dennis Hudson & Smith (1968)	10th Truncation (Present)
1	0.849	0.812	0.805
2	—	1.023	1.012
4	—	1.318	1.298
5	1.426	—	1.410
7	—	1.633	1.598
10	1.864	1.897	1.821
15	2.193	—	2.176
20	—	2.557	2.433
30	—	—	2.850
40	3.255	3.480	3.200

The average Nusselt numbers are shown in Fig. 10 along with earlier experimental data. The results from the present study agree well with the data of Collis and Williams [5] and King [13]. The present result lies slightly below the data of Hilpert [9], Kennelly and Sanborn [11], and Kennelly, Wright, and van Bylevett [12].

7. Conclusions

Nusselt numbers are in good agreement with those of Collis and Williams and Eckert and Soehngen. The results of Collis and Williams and King for the average

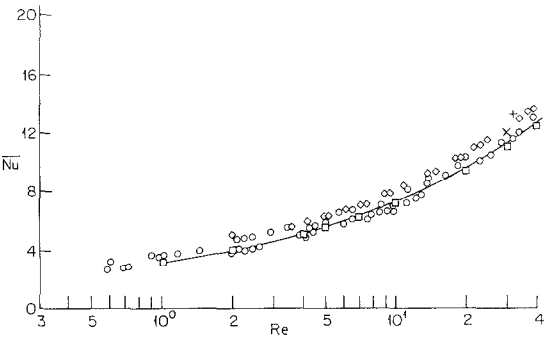

FIG. 10. Comparison of average Nusselt number from the tenth trucation versus Reynolds number (Pr = 0.72) with different experiments: (×), Kennelly *et al.* (1909); (+), Kennely and Sanborn (1914); (○), King (1914); (◇), Hilpert (1933); (□), Collis and Williams (1959); (—) tenth truncation (present).

Nusselt number have also shown satisfactory agreement with the result of the present work. The good agreement in this work could be attributed to the fact that the Nusselt number depends only on the slope of the flow temperature at the wall and not the detailed temperature distribution which is also the case in integral methods.

One of the most crucial tasks in computational fluid dynamics is the selection of the outer velocity boundary conditions. To overcome the limitation of the finite computational domain, we recommend the employment of the Navier–Stokes solutions at large distances from a 2-dimensional finite body obtained by Chang [3] as the velocity boundary conditions. For steady, incompressible, laminar flow over 3-dimensional bodies, the velocity boundary conditions at large distances may be obtained from the asymptotic solutions of Childress [4], although the 3-dimensional relief effects could reduce their importance. It is worthwhile to obtain asymptotic solutions for compressible, and/or turbulent flows to be used as velocity boundary conditions for such flows. The reason is that the region in computing unbounded flow over a finite body is always finite. On the other hand, as the present computation shows, the free-stream temperature boundary condition is quite adequate.

REFERENCES

1. C. J. APELT, Aero. Res. Counc., R & M No. 317, 1958 (unpublished).
2. C. J. APELT AND M. A. LEDWICH, *J. Fluid Mech.* **95**, 761 (1979).
3. I. D. CHANG, *J. Math. Mech.* **10**, 811 (1961).
4. S. CHILDRESS, Jet Propulsion Laboratory California Institute of Technology, Technical Report No. 32–480, 1964 (unpublished).
5. D. C. COLLIS AND M. J. WILLIAMS, *J. Fluid Mech.* **6**, 357 (1959).
6. S. C. R. DENNIS, J. D. HUDSON, AND N. SMITH, *Phys. Fluids* **11**, 933 (1968).
7. E. R. G. ECKERT AND E. SOEHNGEN, *Trans. ASME* **74**, 343 (1952).
8. B. FORNBERG, *J. Fluid Mech.* **98**, 819 (1980).
9. R. HILPERT, *Forschg. Ing.-Wes.* **4**, 215 (1933).
10. H. JAFROUDI AND H. T. YANG, *J. Comput. Phys.* **49**, 181 (1983).
11. A. E. KENNELLY AND H. S. SANBORN, *Proc. Amer. Phil. Soc.* **53**, 55 (1914).
12. A. E. KENNELLY, C. A. WRIGHT, AND J. S. VAN BYLEVETT, *Trans. Amer. Inst. Electr. Eng.* **28**, 363 (1909).
13. L. V. KING, *Philos. Trans. Roy. Soc. London, A* **214**, 373 (1914).
14. T. OJIKA, *The Scientific Subroutine Library*, (Kyoto University, Japan, 1978).
15. Y. TAKAISI, *Phys. Fluids, Suppl.* **12**, II–86 (1969).